ELSEVIER

International Journal of Heat and Fluid Flow 21 (2000) 582–588

International Journal of HEAT AND FLUID FLOW

www.elsevier.com/locate/ijhff

Experimental study on microbubbles and their applicability to ships for skin friction reduction

Yoshiaki Kodama *, Akira Kakugawa, Takahito Takahashi, Hideki Kawashima

Ship Research Institute, 6-38-1, Shinkawa, Mitaka, Tokyo 181-0004, Japan

Abstract

Microbubble experiments were carried out using a circulating water tunnel specially designed for microbubble experiments. The tunnel has a long test section, which enables measurements on the persistence of the skin friction reduction effect by microbubbles in the streamwise direction. It also has a damp tank, which enables continuous testing of microbubbles. Skin friction was measured using a skin friction sensor, which is a force gauge type of 250 N/m^2 full scale, and skin friction reduction by microbubbles up to 40% was obtained. The local void ratio in the bubble condition was measured by putting a suction tube in the test section, and it was obtained that the local void ratio close to the wall has strong correlation with skin friction reduction. The scale effect and the applicability of microbubbles to full scale ships was discussed, based on experimental results using a long flat plate. © 2000 Begell House Inc. Published by Elsevier Science Inc. All rights reserved.

Keywords: Microbubble; Void ratio; Skin friction reduction; Ship

1. Introduction

Ships that carry heavy loads such as crude oil, ore and grain, play an important role in worldwide transportations. Their characteristics are that they are very large and that they move very slowly. Among major drag components of such ships, the free-surface wave component, being proportional to the square of the ship speed, is very small due to their low speed. Therefore the skin frictional drag component occupies approximately 80% of the total drag, thus its reduction is very important.

Skin friction reduction of full-scale ships has its own difficulties. One is that the Reynolds number is very high. Table 1 shows the dimensions of a typical tanker with 150 000 tonnage. The table also shows the height h of riblets, a typical skin friction reduction device, if they are applied to model- and full-scale ships, by assuming that their height corresponds to $h^+ = 15$. If one uses the local skin friction formula (Schlichting, 1968), which is based on the 1/7 power law velocity distribution

$$C_f' \equiv \frac{\tau_w}{(1/2)\rho U^2} = (2\log_{10} R_x - 0.65)^{-2.3}, \tag{1}$$

where R_x is the Reynolds number based on the distance from the leading edge, the height of riblets h is expressed as

$$\frac{h}{L} = h^+ \frac{\sqrt{2}}{R_e}(2\log_{10} R_x - 0.65)^{1.15} \tag{2}$$

and the value h in the table is derived. It is seen that skin friction devices that scale with friction velocity such as riblets, become more difficult to apply as the body size becomes larger. It should also be mentioned that there is a fouling problem in the sea environment, which makes the application still more difficult.

Microbubbles, i.e. small bubbles injected into the boundary layer on a solid wall, reduce skin friction significantly, and have been studied intensively (e.g. Merkle and Deutsch, 1990) since the pioneering works by McCormick and Bhattacharyya (1973), and Bogdevich et al. (1977). Recently several experimental studies on the mechanism of skin friction reduction by microbubbles were carried out (Kato et al., 1994; Guin et al., 1996; Takahashi et al., 1997; Kato et al., 1998).

There are some points that suggest that microbubbles are suited to full-scale ships; (1) there is at least no evidence that shows that microbubbles scale with h^+, and in most cases their experimental results are plotted using the boundary layer thickness or the channel half width (e.g. Merkle and Deutsch, 1990), (2) they are perhaps rather insensitive to fouling, except for air injection holes, and (3) practical hull forms of ships have a wide flat bottom, along which the bubbles injected in the front part can stay close to the flat bottom by buoyancy. Although the skin friction reduction by microbubbles is significant, being up to 80% (e.g. Merkle and Deutsch, 1990), the energy needed for bubble injection is not small because those large ships have water depth of about 20 m resulting in the pressure increase of 2 atms against which bubbles have to be

* Corresponding author. Tel.: +81-422-41-3041; fax: +81-422-41-3053.

E-mail address: kodama@srimot.go.jp (Y. Kodama).

0142-727X/00/$ - see front matter
PII: S0142-727X(00)00048-5

Notation

C_f	skin friction coefficient
U	average flow speed in the test section of the circulating water tunnel
τ_w	wall shear stress
ρ	water density
g	gravity constant
L	length
R_x	Reynolds number based on the distance from the leading edge
R_e	Reynolds number based on the overall length L
h^+	height of a riblet normalized by the skin friction velocity
F_n	Froude number
Q_a	amount of air injected in the test section per unit time
Q_w	amount of water going through the test section per unit time
r	hydraulic radius
α_a	local void ratio in the test section
$\bar{\alpha}_a$	average void ratio in the test section

Table 1
Estimated riblet heights for a 150 000 tonnage tanker[a]

Dimensions	Full-scale ship	Model scale ship
Length L (m)	320	7
Breadth B (m)	60	1.31
Depth d (m)	22	0.48
Speed U (m/s)	7.5	1.11
$R_e(\equiv UL/\nu)$	2.4×10^9	7.8×10^6
h/L	2.38×10^{-7}	5.0×10^{-5}
h (mm)	0.08	0.35

[a] Froude number $F_n \equiv U/\sqrt{gL} \equiv 0.134$, $h^+ \equiv 15$.

injected. Therefore it is necessary to reduce the amount of air and/or increase the drag reduction by studying the drag reduction mechanism and minimizing the amount of injected air.

The scale effect is perhaps the most important factor in the discussion on the applicability of microbubbles to full-scale ships, considering their large size. Since most of previous experimental works were carried out using circulating water tunnels whose test section length is a few meters at most, it was difficult to do such discussions. But recently, large-scale microbubble experiments were carried out in towing tanks. Watanabe et al. (1998) carried out a microbubble experiment using a 40 m-long flat plate ship, and Takahashi et al. (1999) carried out a similar experiment using a 12 m-long flat plate ship. In this paper, some recent experimental results on microbubbles carried out in a small circulating water tunnel will be given, followed by some discussions on the scale effect.

2. Experiments

2.1. Test facility

A closed circulating water tunnel was specially designed for microbubble (Fig. 1). Bubbles are generated by injecting air in the test section. They are removed by buoyancy in a dump tank located downstream of the test section, thus making continuous operation possible.

The width and height of the test section are 100 and 15 mm, respectively, and therefore the flow is almost two-dimensional. The length of the test section is 3000 mm. Since one of the major purposes of this facility is to obtain the data on the persistance of the skin friction reduction effect by microbubbles in the streamwise direction, this rather large length was chosen.

As shown in Fig. 2, bubbles are generated in the air injection chamber by injecting air through a porous plate made of sintered bronze with nominal pore radius of 2 μm. The chamber is located at 1038 mm from the upstream end of the test section, so that the flow is fully developed there. This location is called Position 1, followed by Positions 2, 3, and 4, each 500 mm apart, where various measurements were carried out. It may be stated that the flow in the test section between Position 1 and Position 4, where the bubble generation and all the measurements described in this paper were made, is fully developed, and therefore the half height of the channel corresponds to the boundary layer thickness of outer flows.

The amount of injected air is expressed by the average volume ratio $\bar{\alpha}_a$ defined as

$$\bar{\alpha}_a \equiv \frac{Q_a}{Q_a + Q_w}, \tag{3}$$

where Q_a: volumetric flow rate of air in the test section; Q_w: volumetric flow rate of water in the whole test section of 100 mm × 15 mm.

2.2. Skin friction measurement

The skin friction was measured in the test section with or without bubbles using skin friction sensors (Sankei Engineering) shown in Fig. 3. The sensor is a force gauge type (Kato et al., 1994) with a sensing disk, which has a diameter of 10 mm and the maximum load of 2 g weight, resulting in 250 N/m^2 full

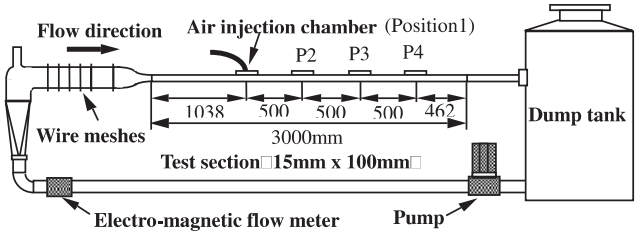

Fig. 1. A circulating water tunnel for microbubble experiments.

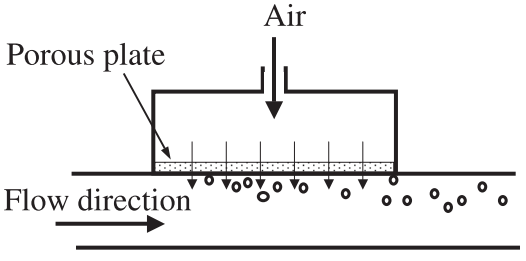

Fig. 2. Air injection chamber and bubble generation through a porous plate.

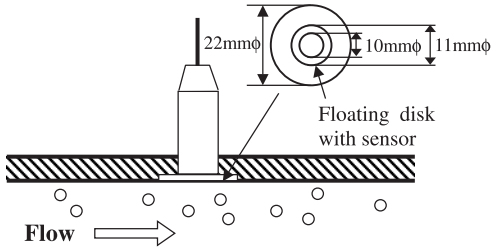

Fig. 3. Skin friction sensor.

scale. The sensors were placed on the center plane of the test section.

2.2.1. Calibration

Static and dynamic calibration of the skin friction sensors was made. In the static calibration the sensor axis was held horizontally, and the weights of up to 2 g were attached on the sensing disk using adhesive tape. The calibration was made with two sensors, and the calibration constants thus obtained were compared with the ones supplied by the manufacturer. It was found that the two kinds of constants agreed within 3% and 5%, and thus the calibration constants by the manufacturer were used thereafter.

In the dynamic calibration, the sensor was mounted flush on the upper wall surface of the test section, and the skin friction was measured in the non-bubble condition at various flow speeds. The result is shown in Fig. 4, in which the Blasius empirical formula (Schlichting, 1968) and the results based on the measured pressure gradients are also shown. The pressure gradients were obtained by measuring pressure drops between Position 1 and Position 3, while the sensor was placed at Position 2 (see Fig. 1). The results by the skin friction sensors, obtained on three different dates, show some scatter. Although the results by the three methods show consistent deviation among each other, the overall tendency are similar, and it may be stated that this skin friction sensor can measure skin friction with reasonable accuracy.

2.2.2. Correction to C_{f_0}

In the following, the measured skin friction coefficients C_f in the bubble condition are shown as the ratio to that in the non-bubble condition C_{f_0}. In the bubble condition, i.e., when

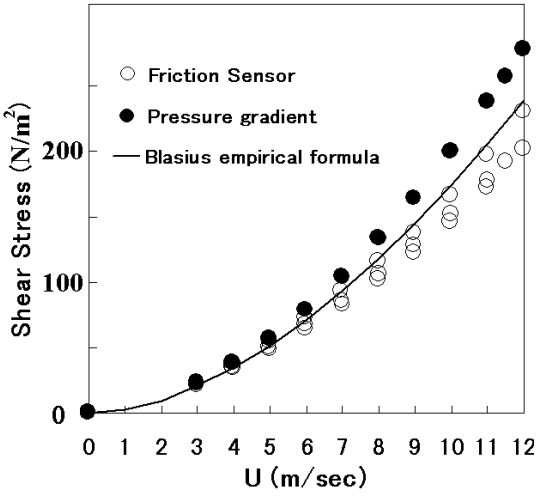

Fig. 4. Dynamic calibration of skin friction sensors.

the air is injected in the test section, the flow speed increases due to the volumetric increase of the flow, and C_{f_0}, the skin friction in the non-bubble condition, needs to be corrected in the bubble condition. Therefore C_{f_0} was corrected as a function of the flow rate of injected air, using the following formulae.

$$C_{f_0}(Q_a) = C_{f_0}(0)\frac{\tau[U(Q_a)]}{\tau[U(0)]}, \tag{4}$$

$$\tau(f) = 0.03325\rho v^{1/4} f^{7/4} r^{-1/4}, \tag{5}$$

where $C_{f_0}(Q_a)$: corrected C_{f_0} at the air flow rate Q_a; $U(Q_a)$: average flow speed at Q_a; r: hydraulic radius.

Eq. (5) corresponds to the empirical Blasius formula (Schlichting, 1968). The above two equations result in multiplying $C_{f_0}(0)$ with $[U(Q_a)/U(0)]^{7/4}$.

2.2.3. Measured results

The skin friction was measured at three speeds of $U = 5$, 7, and 10 m/s, at Positions 2, 3, and 4. The results are shown in Fig. 5. Dotted lines show an empirical formula obtained by Merkle and Deutsch (1990)

$$\frac{C_f}{C_{f_0}} = 0.8e^{-4\bar{\alpha}_a} + 0.2. \tag{6}$$

It should be noted that the Q_a values were calculated using the local pressure at each measurement location because there was non-negligible streamwise pressure gradient due to head loss in the test section.

At all the three speeds, the skin friction reduction increased as the amount of injected air increased. The maximum skin friction reduction was approximately 30%, while that of Merkle's experimental data on which Eq. (6) is based was approximately 80%. It should be mentioned that Merkle's experimental data was obtained at 50–65 mm downstream of the point of bubble injection, and the present data was obtained at 500–1500 mm downstream. At $U = 5$ m/s the present skin friction reduction values agree rather well with Eq. (6), but at higher speeds the reduction becomes smaller and the agreement with Eq. (6) becomes poorer, which might suggest that the correction using Eq. (4) is reasonable but not good enough. Based on the finding by Deutsch and Clark (1988), another possible explanation for the smaller skin friction reduction at higher speed is the favorable pressure gradient due to the head loss in the channel, which becomes greater at higher speed.

In Fig. 6, the streamwise distribution of skin friction reduction at $\bar{\alpha}_a = 0.08$ is plotted. The skin friction reduction is generally insensitive to streamwise locations. At $U = 10$ m/s the skin friction reduction at Position 2 is greater than those at the other two locations.

2.3. Local void ratio measurement

In order to find out the relation between the skin friction reduction and the void ratio, the local void ratio α_a was measured using a suction tube system (Fig. 7) similar to the one used by Guin et al. (1996). A small tube with 1.2 mm inner diameter and 1.6 mm outer diameter was placed in the test section. The tube was connected to a vacuum pump for suction via two chambers to measure the volumes of collected air and water separately. The suction pressure was adjusted so that, in the non-bubble condition, the volume of the collected water was equal to that which passed through the suction area of the tube when the tube was not present in the flow. This means that the suction pressure was adjusted at each distance from

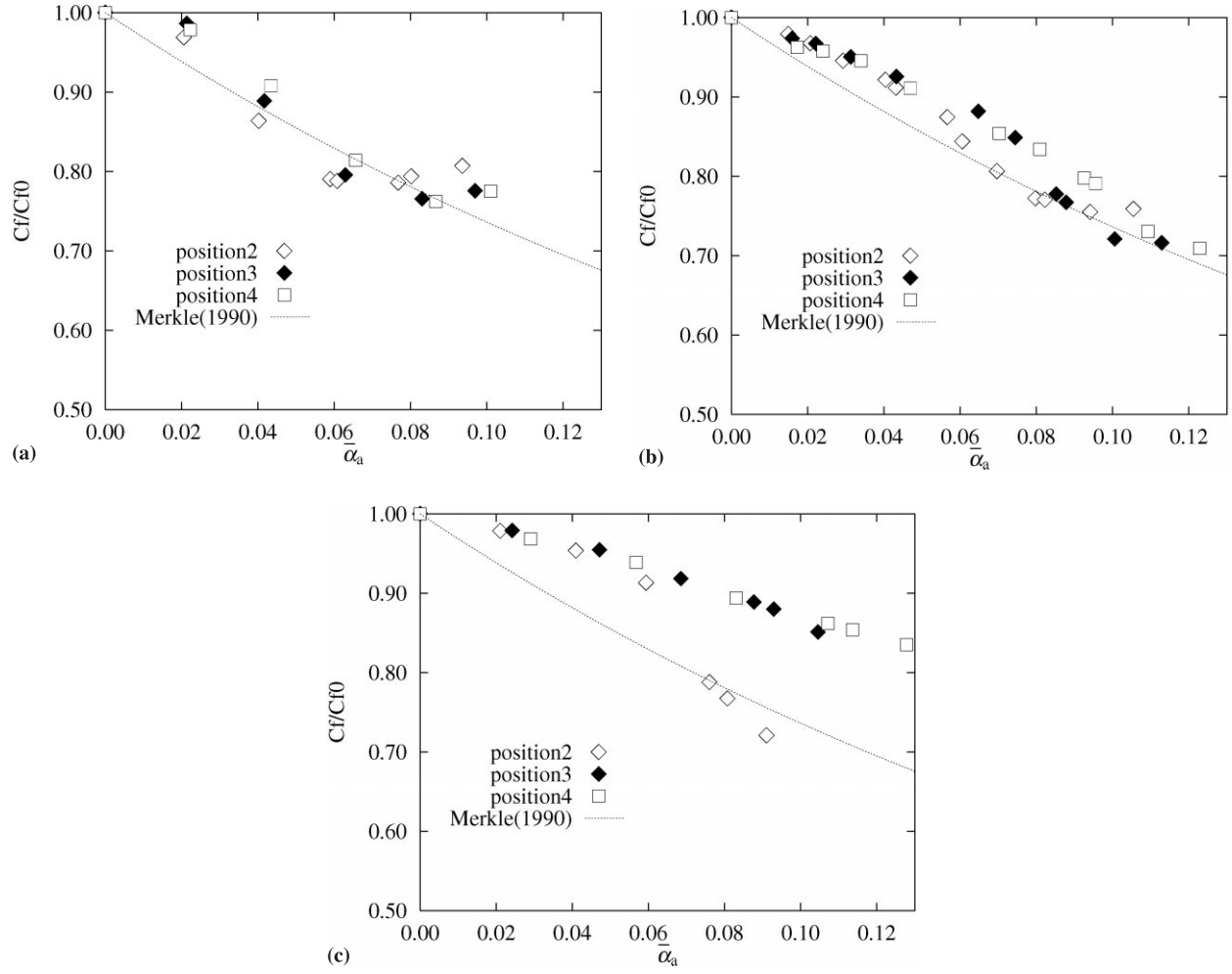

Fig. 5. Skin friction reduction by microbubbles (porous plate): (a) $U = 5.0$ m/s; (b) $U = 7.0$ m/s; (c) $U = 10.0$ m/s.

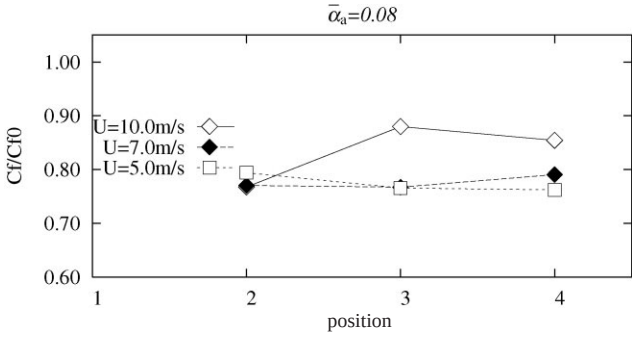

Fig. 6. Streamwise distribution of skin friction reduction ($\bar{\alpha}_a = 0.08$, porous plate).

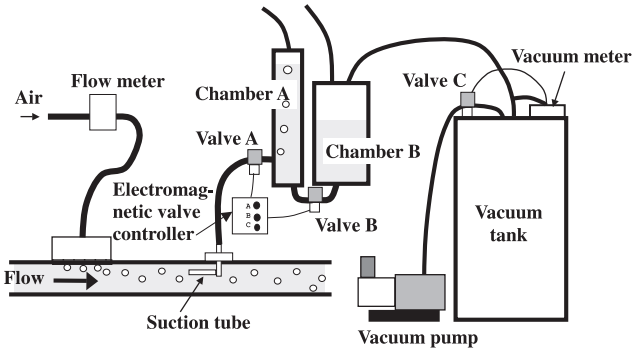

Fig. 7. Suction tube to measure local void ratio.

the wall, and due to the pressure drop in the streamwise direction, at each streamwise location.

The measurements were made at $\bar{\alpha}_a = 0.08$ and at the flow speed $U = 5$, 7, and 10 m/s. At $U = 5$ and 7 m/s, the suction pressure was adjusted in the way described above, but at $U = 10$ m/s the pressure was fixed at 0.105 atm (80 mmHg) because the low pressure in the downstream positions made the adjustment described above impossible. The measured local void ratio α_a was integrated in the test section by assuming uniform distribution in the spanwise direction. At $U = 5$ m/s the integrated air flow rate thus obtained was 1.61–2.04 times that measured with the flow meter at the injection point, at $U = 7$ m/s it was 1.42–1.56 times, and at $U = 10$ m/s it was 0.72–0.99 times. A possible explanation for the discrepancy at two lower speeds is that the bubbles distribute more densely in the center.

The measured local void ratio α_a was corrected by multiplying a constant so that the integrated air flow rate becomes equal to that at the point of injection. It should be noted that $\bar{\alpha}_a$ is defined at the point of injection (Position 1) and that the

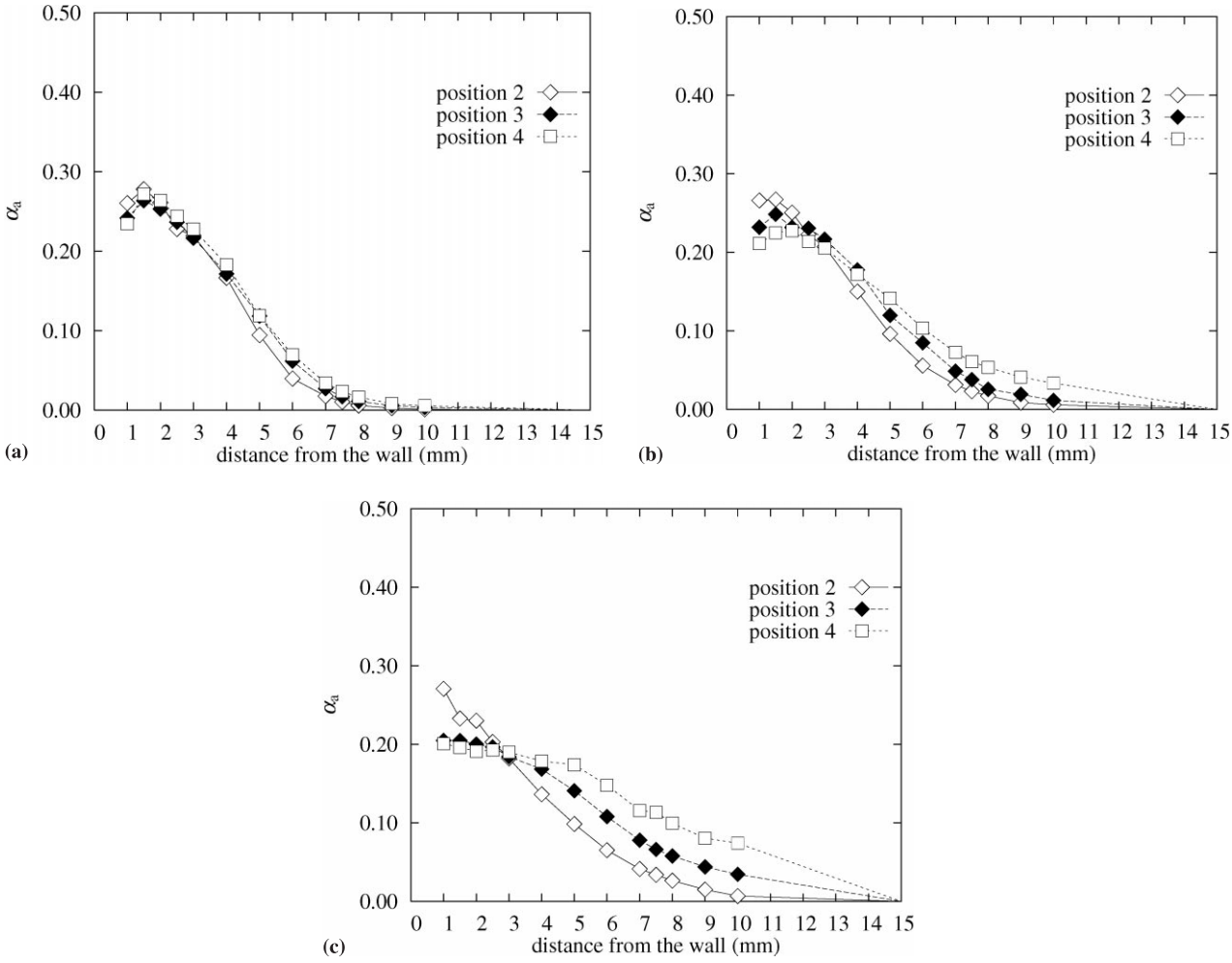

Fig. 8. Local void ratio α_a ($\bar{\alpha}_a = 0.08$, porous plate, corrected): (a) $U = 5.0$ m/s; (b) $U = 7.0$ m/s; (c) $U = 10.0$ m/s.

volume of injected air increases toward downstream because of the pressure drop, which is greater at higher speed. The results are shown in Fig. 8. At $U = 5$ m/s, the bubbles are clustered near the wall surface and hardly diffuse at downstream locations. They diffuse at $U = 7$ and 10 m/s, and the degree of diffusion is greater at the higher speed. At $U = 10$ m/s, the bubbles diffuse significantly at downstream locations. When one plots the skin friction reduction shown in Fig. 6 and the maximum value of the local void ratio $\alpha_{a_{max}}$, which usually occurs close to the wall, they seem to have correlation, i.e., the skin friction reduction becomes greater as $\alpha_{a_{max}}$ becomes greater (Fig. 9). This agrees with the findings by many investigators including Pal et al. (1988). Other possible factors for the skin friction reduction such as bubble size (e.g. see Gore and Crowe, 1989) is beyond the scope of this paper.

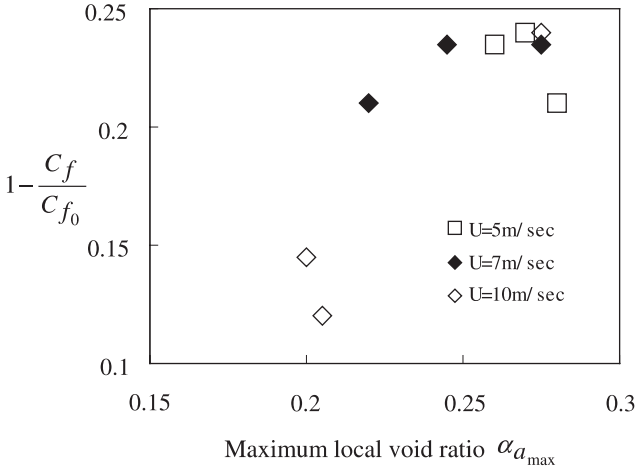

Fig. 9. Maximum local void ratio $\alpha_{a_{max}}$ and skin friction reduction $1 - C_f/C_{f_0}$.

2.4. Array-of-holes plate

The porous plate used to generate bubbles has some problems. One is that only the nominal size of the holes is known. The other is the non-uniformity of the generated bubbles, i.e., one can easily observe that the size and number of the generated bubbles is not uniformly distributed on the porous plate. The third problem is that the pressure loss is not nominal.

In order to solve these problems, a new plate called array-of-holes plate was manufactured. On the plate, holes of 1 mm diameter were made at the intervals of 5 mm in the streamwise direction and 3 mm in the spanwise direction. Using the array-of-holes plate, skin friction was again measured, and the results

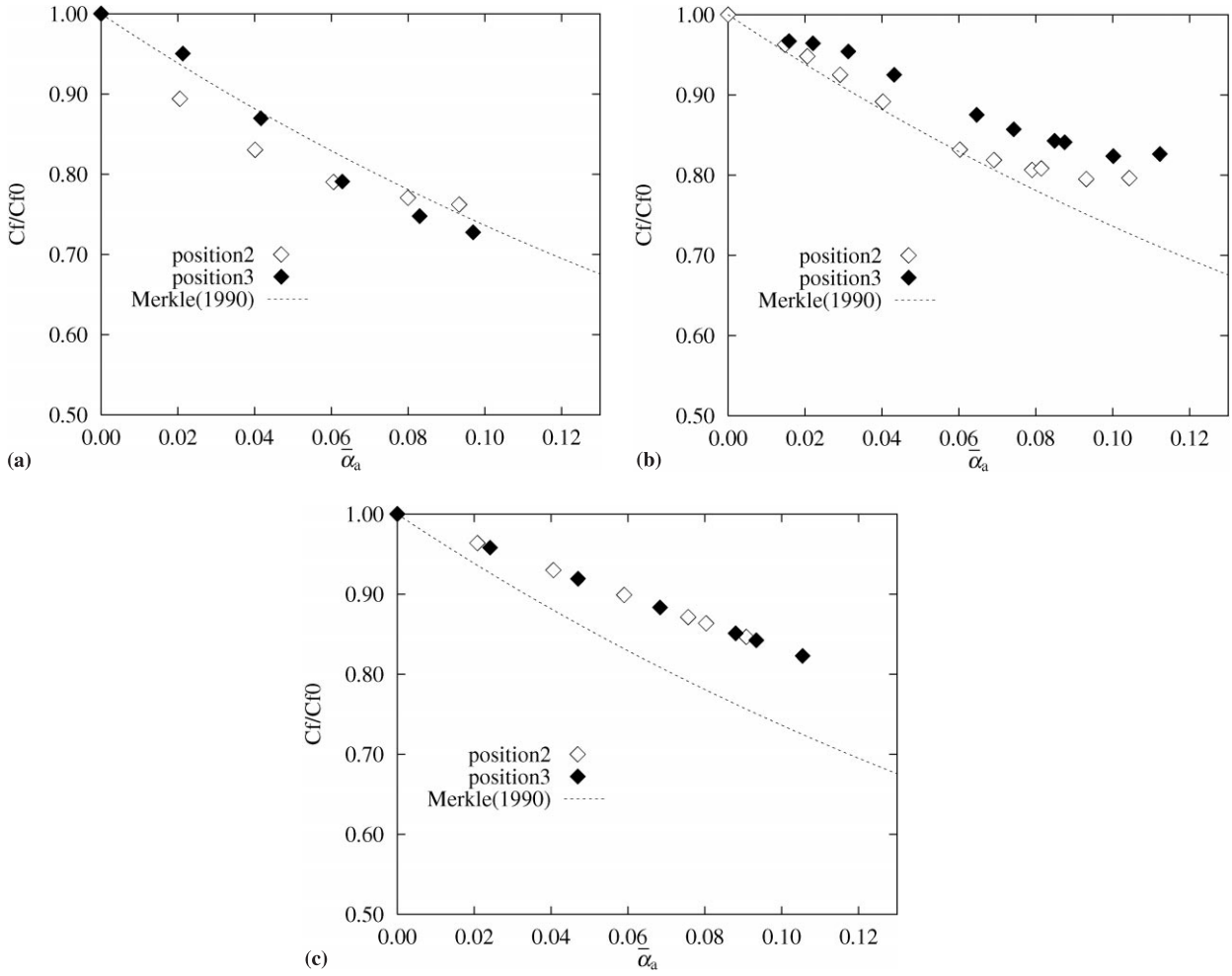

Fig. 10. Skin friction reduction by microbubbles (array-of-holes plate): (a) $U = 5.0$ m/s; (b) $U = 7.0$ m/s; (c) $U = 10.0$ m/s.

are shown in Fig. 10. Comparing Fig. 10 with Fig. 5, it is seen that skin friction reduction by the array-of-holes plate is comparable to that by the porous plate, except for the result at $U = 10$ m/s and at Position 2, in which the skin friction reduction is much greater at higher void ratio using the porous plate, while that using the array-of-holes plate is comparable to others.

3. Applicability of microbubbles to ships

In order to apply microbubbles to full-scale ships, net drag reduction must be achieved. That is, the energy saved by skin friction reduction must be at least larger than the energy spent to generate bubbles against the hydrostatic pressure at the bottom of a ship. Merkle and Deutsch (1990) discussed the net drag reduction of microbubbles to ships based on the experimental data of skin friction reduction described as Eq. (6), by defining the water flow rate Q_w as

$$Q_w = Ub(\delta - \delta^*), \tag{7}$$

where b is the boundary layer width, δ is the boundary layer thickness and δ^* is the displacement thickness. This relation assumes that the boundary layer thickness is the representative length of this phenomenon.

Watanabe et al. (1998) measured, in their towing tank, the skin friction reduction by microbubbles on a flat plate 20 or 40 m long and 0.6 m wide, using skin friction sensors similar to those used in the present study. The result is shown in Fig. 11. Bubbles were injected through a porous plate 250 mm wide located at 1.2 m from the front end. The speed was 7 m/sec. The air flow rate was 1.7×10^3 m^3/s, 3.3×10^3 m^3/s, and 5.0×10^3 m^3/s. The three curves show the general tendency of

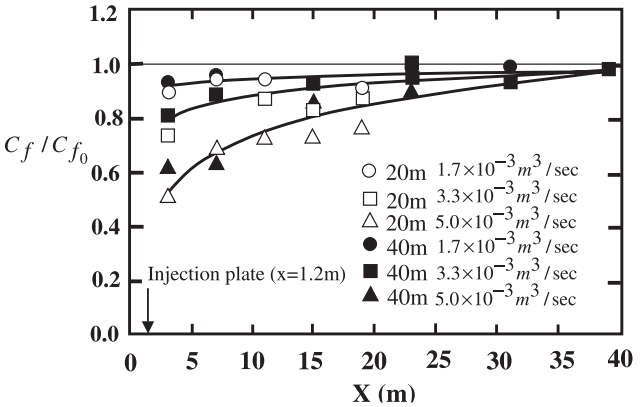

Fig. 11. Skin friction reduction by microbubbles on 20 and 40 m flat plates (Watanabe, 1998): $U = 7$ m/s, $Q_a = 1.7$, 3.3, and 5.0×10^{-3} m^3/s.

Table 2
Estimated C_f/C_{f_0} using Eq. (6) and 1/7 power law[a]

Distance from LE (m)	10	20	40
δ (m)	0.0998	0.174	0.303
$\bar{\alpha}_a$	0.0317	0.0184	0.0107
C_f/C_{f_0}	0.91	0.94	0.97

[a] $Q_a = 0.005$ m^3/s, $U = 7$ m/s, and $b = 0.25$ m.

the three sets of data. If the Eq. (7) is used to calculate Q_w, and the 1/7 power law is used for the boundary layer development, the Eq. (6) gives the skin friction ratio C_f/C_{f_0} shown in Table 2 at $Q_a = 0.005$ m^3 and $U = 7$ m/s. It is seen that the skin friction reduction shown in Fig. 11 is much greater than that in Table 2. The authors suspect that this discrepancy means that the boundary thickness is not a proper length scale for this phenomenon. Further studies on the scale effect of microbubbles are clearly needed.

4. Conclusions

Microbubbles were studied experimentally using a circulating water tunnel specially designed for the tests. The skin friction reduction by microbubbles was measured directly using skin friction sensors at three speeds of $U = 5$, 7, and 10 m/s. The reduction was greater at larger air injection rate and at lower speed. The local void ratio distribution in the boundary layer was measured using a suction tube system. The results agreed with the finding by many investigators, i.e. the local void ratio close to the wall is important for skin friction reduction by microbubbles. Two types of plates used for bubble injection, i.e. a porous plate with nominal pore radius of 2 μm and a plate with 1 mm diameter holes in arrays. They produced similar skin friction reduction effects, the former being slightly better. The skin friction reduction by microbubbles measured on a 40 m-long flat plate ship (Watanabe et al., 1998) was much greater than that estimated using the Merkle and Deutsch (1990)'s empirical formula, which suggests that the average void ratio in the boundary layer is not a proper parameter for scaling the effect. Further studies are needed for clarifying the mechanism of skin friction reduction by microbubbles, especially the scale effect, in order to apply the method to full scale ships.

Acknowledgements

The authors are grateful to Prof. H. Kato of Toyo University for guidance in carrying out the research. This work was carried out in a drag reduction research project (1995–1999) funded by the Ministry of Transport, Japan. A part of the study was carried out in the SR239 project funded by the Ship Research Association, Japan.

References

Bogdevich, V.G., Evseev, A.R., Malyuga, A.G., et al., 1977. Gas saturation effect on near-wall turbulence characteristics. In: Proceedings of the Second International Conference on Drag Reduction, Cambridge, UK, BHRA, pp. 25–37.

Deutsch, S., Clark III, H., 1988. Microbubble skin friction reduction on an axisymmetric body under the influence of applied axial pressure gradients. Phys. Fluids A 3 (12), 2948–2954.

Gore, R.A., Crowe, C.T., 1989. Effect of particle size on modulating turbulent intensity. Int. J. Multiphase Flow 15 (2), 279–285.

Guin, M.M., et al., 1996. Reduction of skin friction by microbubbles and its relation with near-wall bubble concentration in a channel. J. Mar. Sci. Technol., Soc. Naval Arch. Jpn. 1 (5).

Kato, H., et al., 1994. Frictional drag reduction by injecting bubbly water into turbulent boundary layer. In: Cavitation and Gas Liquid Flow in Fluid Machinery and Devices FED, vol.190, ASME, pp. 185–194.

Kato, H., et al., 1998. Effect of microbubble cluster on turbulent flow structure. in: Proceedings of the IUTAM Symposium on Mechanics of Passive and Active Flow Control, Gottingen.

McCormick, M.E., Bhattacharyya, R., 1973. Drag reduction of a submersible hull by electrolysis. Naval Eng. J. 85 (2), 11–16.

Merkle, C., Deutsch, S., 1990. Drag Reduction in Liquid Boundary Layers by Gas Injection. Progress in Astronautics and Aeronautics, vol. 123, AIAA, pp. 351–412.

Pal, S., Merkle, C.L., Deutsch, S., 1988. Bubble characteristics and trajectories in a microbubble boundary layer. Phys. Fluids 31 (4), 744–751.

Schlichting, H., 1968. Boundary-Layer Theory, sixth ed., McGraw-Hill, New York.

Takahashi, T., et al., 1997. Streamwise distribution of the skin friction reduction by microbubbles. J. Soc. Naval Arch. Jpn. 182, 1–8.

Takahashi, T., et al., 1999. Experimental skin friction reduction by microbubbles using a ship with a flat bottom. In: Proceedings of the Turbulence Symposium, Tokyo.

Watanabe, O., et al., 1998. Measurements of drag reduction by microbubbles using very long ship models. J. Soc. Naval Arch. Jpn. 183, 53–63.